

Three-dimensional quantitative structure–activity relationship studies on novel series of benzotriazine based compounds acting as Src inhibitors using CoMFA and CoMSIA

Carlos Gueto, José L. Ruiz, Juan E. Torres, Jefferson Méndez and Ricardo Vivas-Reyes*

*Grupo de Química Cuántica y Teórica, Universidad de Cartagena, Programa de Química,
Facultad de Ciencias Exactas y Naturales Cartagena, Colombia*

Received 17 August 2007; revised 20 November 2007; accepted 21 November 2007
Available online 28 November 2007

Abstract—Comparative molecular field analysis (CoMFA) and comparative molecular similarity indices analysis (CoMSIA) were performed on a series of benzotriazine derivatives, as Src inhibitors. Ligand molecular superimposition on the template structure was performed by database alignment method. The statistically significant model was established of 72 molecules, which were validated by a test set of six compounds. The CoMFA model yielded a $q^2 = 0.526$, non cross-validated R^2 of 0.781, F value of 88.132, bootstrapped R^2 of 0.831, standard error of prediction = 0.587, and standard error of estimate = 0.351 while the CoMSIA model yielded the best predictive model with a $q^2 = 0.647$, non cross-validated R^2 of 0.895, F value of 115.906, bootstrapped R^2 of 0.953, standard error of prediction = 0.519, and standard error of estimate = 0.178. The contour maps obtained from 3D-QSAR studies were appraised for activity trends for the molecules analyzed. Results indicate that small steric volumes in the hydrophobic region, electron-withdrawing groups next to the aryl linker region, and atoms close to the solvent accessible region increase the Src inhibitory activity of the compounds. In fact, adding substituents at positions 5, 6, and 8 of the benzotriazine nucleus were generated new compounds having a higher predicted activity. The data generated from the present study will further help to design novel, potent, and selective Src inhibitors as anticancer therapeutic agents.

© 2007 Elsevier Ltd. All rights reserved.

1. Introduction

The non-receptor protein tyrosine kinase, Src, is a 60-kDa protein that is the archetypal member of a nine-gene family, including Src, Yes, Fyn, Lyn, Lck, Hck, Fgr, Blk, and Yrk, that plays a critical role in regulation of proliferation, differentiation, migration, adhesion, invasion, angiogenesis, and immune function.^{1–4} It has been also well documented that Src protein is overexpressed and/or aberrantly activated in a variety of human tumors, including breast,^{5,6} colon,^{7–9} and pancreatic^{10,11} cancers. For these reasons, interest in development of Src inhibitors has increased sharply over the past several years for their use as potential anticancer therapeutics.¹² Several series of Src inhibitors have been reported to date.^{13–23} Recently, Noronha and coworkers^{24,25} have published novel series of benzotriazine based compounds exhibiting potent Src kinase activity.

Nowadays, three-dimensional (3D) quantitative structure–activity relationship (3D-QSAR) techniques, such as comparative molecular field analysis (CoMFA) and comparative molecular similarity analysis (CoMSIA),^{26–28} are routinely used in modern drug design to help understand drug–receptor interaction. It has been shown in the literature that these computational techniques can strongly support and help the design of novel, more potent inhibitors by revealing the mechanism of drug–receptor interaction.^{29–31} In this study, we have developed predictive 3D-QSAR models using benzotriazine derivatives, which have been reported as Src kinase inhibitors.^{24,25}

2. Data sets

In vitro inhibitory activity data (IC₅₀, μ M) of a series of benzotriazine based compounds, reported by Noronha

Keywords: Benzotriazine; CoMFA; CoMSIA; Src inhibitors; Bioinformatic.

*Corresponding author. Tel./fax: +57 5 6698180; e-mail: rvivasr@unicartagena.edu.co

et al.,^{24,25} were taken for the study. Out of 109 Src inhibitors which were reported, either molecules whose IC₅₀ values were not quantitatively reported or redundant structures were not considered for the study. The total set of Src kinase inhibitors (78 compounds) was divided into training (72 compounds) set to generate the 3D-QSAR models (Tables 1–4) and test (6 compounds) set to evaluate the predictive power of the resulting models (Tables 1–4). The test compounds were selected manually such that the structural diversity and wide range of activity in the data set were included. Src kinase inhibitory activities were converted into the corresponding pIC₅₀ (–log IC₅₀) values and used as dependent variables in the CoMFA and CoMSIA analyses.

3. Molecular modeling

All molecular modeling studies were performed using the molecular modeling package SYBYL7.0.³² CoMFA and CoMSIA studies require that the 3D structures of the molecules to be analyzed are aligned according to a suitable conformational template, which is assumed to be a bioactive conformation.³³ Though, due to the fact that bioactive conformations of these inhibitors are not known, the lowest energy conformations were reasonable initial structures to perform 3D-QSAR calculations. Energy minimizations were performed using the Tripos force field²⁶ and the Gasteiger–Huckel³⁴ charge with a distance-dependent dielectric and conjugate gradient method. The criterion of convergence was 0.05 kcal/mol. Subsequently, the lowest-energy conformation found for each structure was submitted to

optimization with the semiempirical AM1 method³⁵ by means of the Gaussian 94 Software.³⁶

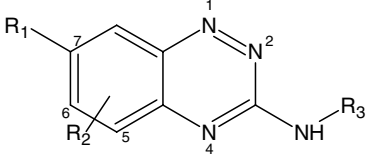
4. Compound alignment

One of the most important adjustable parameters in 3D-QSAR is the relative alignment of all the molecules to one another so that they have a comparable conformation and a similar orientation in space.³⁷ The most active and pharmacokinetically stable compound **20**²⁵ was used as a template for superimposition, assuming that its conformation represents the most bioactive conformation of the benzotriazine derivatives at the enzyme active site level. Each analog was aligned to the template by rotation and translation so as to minimize the RMSD between atoms in the template and the corresponding atoms in the analog using the DATABASE ALIGN option in SYBYL. The common fragment shown in Figure 1 and the aligned compounds are displayed in Figure 2.

5. CoMFA and CoMSIA models

The aligned training set molecules were placed in a 3D grid box such that the entire set was included in it. The steric (Lennard–Jones 6–12 potential) and electrostatic (Coulomb potential) field energies were calculated using sp³ carbon as probe atom. The energies were truncated to ± 30 kcal mol^{–1}. The CoMFA fields generated automatically were scaled by the CoMFA-STD method in SYBYL.

Table 1. Structures and biological activities of the training and test sets of molecules

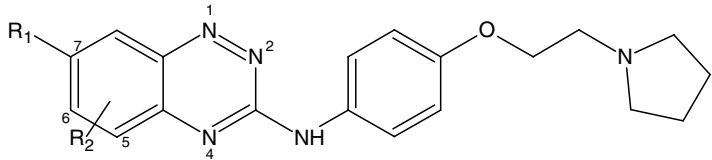


Compound	R ₁	R ₂	R ₃	Actual ^a	CoMSIA ^b		CoMFA	
					Pred	δ	Pred	δ
1	2,6-Cl ₂ Ph	5-Me	H	–0.556	–0.025	–0.531	–0.435	–0.121
2	2-Naphthyl	H	H	–0.716	–1.165	0.449	–1.768	1.052
3	2,6-Me ₂ Ph	H	H	–0.342	–0.079	–0.263	–0.193	–0.149
4	2,6-Me ₂ Ph	5-Me	H	–0.869	–0.009	–0.860	–0.155	–0.714
5	2-Cl-5-OH Ph	5-Me	H	–0.176	–0.773	0.597	–0.870	0.694
6	2,6-Me ₂ Ph	H	Ph	–0.176	0.349	–0.525	0.647	–0.823
7 ^c	2,6-Me ₂ Ph	5-Me	Ph	0.387	0.423	–0.036	0.700	–0.313
8	2,6-Me ₂ Ph	5,6-Me ₂	Ph	0.886	0.567	0.319	0.750	0.136
9	2,6-Me ₂ Ph	5-Me	3-ClPh	0.886	0.297	0.589	0.842	0.044
10	2,6-Me ₂ Ph	5-Me	4-N(Me) ₂ Ph	0.620	0.815	–0.195	0.834	–0.214
11	2,6-Me ₂ Ph	5-Me	4-MeOPh	0.854	0.999	–0.145	0.919	–0.065
12 ^c	2,6-Me ₂ Ph	5-Me	4-EtOPh	0.959	1.193	–0.234	1.4	–0.345
13	2,6-Me ₂ Ph	5-Me	3-Me Ph	0.745	0.391	0.354	0.854	–0.109
14	2,6-Me ₂ Ph	5-Me	3,4-Me ₂ Ph	0.018	0.265	–0.247	0.890	–0.872
15	2,6-Me ₂ Ph	5-Me	3-SO ₂ NH ₂ Ph	0.854	0.881	–0.027	0.913	–0.059
16	2,6-Me ₂ Ph	5-Me	4-Pyridyl	1.398	1.145	0.253	0.616	0.782
17	2,6-Me ₂ Ph	5-Me	COPh	–0.255	–0.069	–0.186	0.033	–0.288

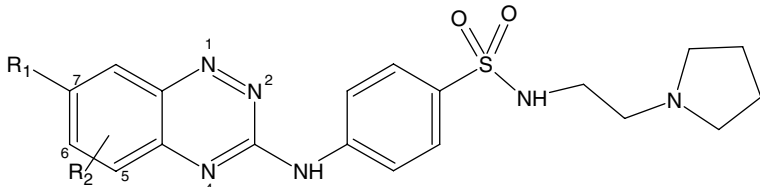
^a Biological activity ($\mu\text{mol L}^{-1}$) expressed as $-\log\text{IC}_{50}$ against human Src enzyme.

^b Calculated activity from alignment VII.

^c Test set molecules.

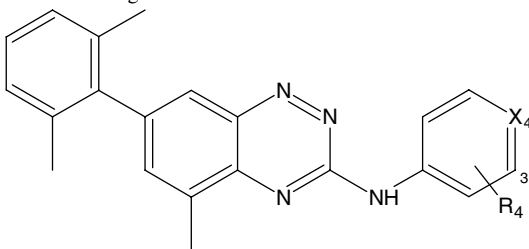
Table 2. Structures and biological activities of the training and test sets of molecules


Compound	R ₁	R ₂	Actual ^a	CoMSIA ^b		CoMFA	
				Pred	δ	Pred	δ
18	2,6-Me ₂ Ph	5-Me	2.155	1.887	0.268	1.629	0.526
19	Ph	5-Me	0.467	0.642	−0.175	0.520	−0.053
20	2,6-Cl ₂ Ph	5-Me	1.959	1.777	0.182	1.179	0.780
21	2-Cl Ph	5-Me	1.456	1.156	0.300	0.871	0.585
22	2,6-F ₂ Ph	5-Me	0.682	0.659	0.023	0.458	0.224
23	2-Cl,6-OMe Ph	5-Me	0.297	0.435	−0.138	1.072	−0.775
24	2-Cl,5-OMe Ph	5-Me	0.109	0.378	−0.269	0.118	−0.009
25	3-Cl,6-OMe Ph	5-Me	−0.079	0.138	−0.217	0.409	−0.488
26	4-(2-F, 5-Me pyridyl)	5-Me	0.690	0.650	0.040	0.710	−0.020
27	4-(3,5-Me ₂ isoxazole)	5-Me	0.684	0.425	0.259	0.907	−0.223
28	4-Pyrimidyl	5-Me	−0.176	−0.129	−0.047	0.008	−0.184
29 ^c	2-Pyridyl	5-Me	−0.255	−0.097	−0.158	0.149	−0.404
30	2,6-Me ₂ Ph	H	1.824	1.799	0.025	1.564	0.260
31	2,6-Cl ₂ Ph	H	1.523	1.688	−0.165	1.132	0.391
32	2,6-Me ₂ Ph	6-Me	1.921	1.920	0.001	1.623	0.298
33	2,6-Me ₂ Ph	NH ₂	2.000	2.058	−0.058	1.692	0.308
34 ^c	2,6-Me ₂ Ph	NHMe	2.000	2.095	−0.095	1.709	0.291
35	2,6-Me ₂ Ph	NHCOCH ₃	1.854	1.967	−0.113	1.570	0.284
36	2,6-Me ₂ Ph	NHSO ₂ Me	1.678	1.860	−0.182	1.622	0.056

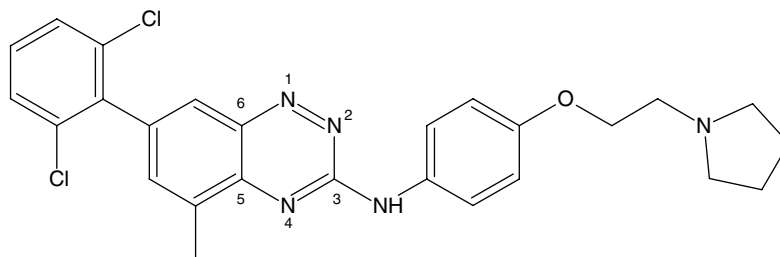
^a Biological activity (μmol L^{−1}) expressed as −logIC₅₀ against human Src enzyme.^b Calculated activity from alignment VII.^c Test set molecule.**Table 3.** Structures and biological activities of the training and test sets of molecules


Compound	R ₁	R ₂	Actual ^a	CoMSIA ^b		CoMFA	
				Pred	δ	Pred	δ
37	2,6-Me ₂ Ph	5-Me	2.046	1.991	0.055	1.883	0.163
38 ^c	2,6-Cl ₂ Ph	5-Me	1.854	1.951	−0.097	1.533	0.321
39	2-Cl,6-OH Ph	5-Me	1.886	1.370	0.516	1.637	0.249
40	3-CN,6-Me Ph	5-Me	1.602	1.523	0.079	1.445	0.157
41	3-NH ₂ ,6-Cl Ph	5-Me	1.292	0.714	0.578	0.667	0.625
42	3-NH ₂	5-Me	0.550	0.222	0.328	0.344	0.206
43	3-CH ₂ NH ₂ ,6-Me Ph	5-Me	0.452	0.756	−0.304	1.213	−0.761
44	3-NHMe Ph	5-Me	0.200	0.337	−0.137	0.468	−0.268
45	3-NHSO ₂ Me Ph	5-Me	−0.462	−0.301	−0.161	−0.060	−0.402
46	2,6-Me ₂ Ph	6-Me	1.959	2.091	−0.132	1.999	−0.040
47	Ph	6-Me	0.502	1.147	−0.645	1.084	−0.582
48	2-MePh	6-Me	2.000	1.671	0.329	1.707	0.293
49	2-CF ₃ Ph	6-Me	1.174	1.399	−0.225	1.443	−0.269
50	3-CN,6-Me Ph	6-Me	1.921	1.675	0.246	1.673	0.248
51	4-F,2-Me Ph	6-Me	1.699	1.702	−0.003	1.716	−0.017
52	2-NH ₂	6-Me	1.036	0.834	0.202	1.432	−0.396
53	2-CH ₂ OH Ph	6-Me	1.143	1.122	0.021	1.786	−0.643

^a Biological activity (μmol L^{−1}) expressed as −logIC₅₀ against human Src enzyme.^b Calculated activity from alignment VII.^c Test set molecule.

Table 4. Structures and biological activities of the training and test sets of molecules


Compound	X	R ₄	Actual ^a	CoMSIA ^b		CoMFA	
				Pred	δ	Pred	δ
54	CH	3-(2-Diethylaminoethoxy)	2.000	1.820	0.180	1.745	0.255
55	CH	4-(2-Diethylaminoethoxy)	2.000	1.998	0.002	1.779	0.221
56	CH	4-(4-(2-Ethoxy)morpholino)	1.495	1.720	−0.225	1.638	−0.143
57	CH	3-(2-Morpholin-4-ylethoxy)	1.481	1.375	0.106	1.598	−0.117
58	CH	4-(3-Pyrrolidin-1-yl-propoxy)	1.886	1.906	−0.020	1.655	0.231
59	CH	3-(2-Pyrrolidin-1-yl-ethoxy)	2.194	1.831	0.363	1.846	0.348
60	CH	4-[2-(4-Methyl-piperazin-1-yl)-ethoxy]	1.678	1.700	−0.022	1.287	0.391
61	CH	3-[2-(4-Methyl-piperazin-1-yl)-ethoxy]	1.398	1.463	−0.065	1.346	0.052
62	CH	4-(2-(1-Pyrrolidinyl)ethoxy)	2.155	1.795	0.360	1.578	0.577
63	CH	4-[2-(4-Methyl-piperazin-1-yl)-propoxy]	1.444	1.571	−0.127	1.576	−0.132
64	CH	3-[2-(4-Methyl-piperazin-1-yl)-propoxy]	1.409	1.413	−0.004	1.895	−0.486
65	CH	4-(40-Methyl-piperazin-1-yl)-amido	1.824	2.060	−0.236	1.941	−0.117
66	CH	3-(2-Pyrrolidin-1-yl-ethyl)-sulfonamido	1.585	1.595	−0.010	1.765	−0.180
67 ^c	CH	4-(Piperazin-1-yl)-amido	1.886	2.023	−0.137	1.873	0.013
68	CH	4-(<i>N,N</i> -Dimethylamino)ethylcarboxamido	2.097	2.285	−0.188	2.028	0.069
69	CH	4-(<i>N</i> -(2-Pyrrolidin-1-yl-ethyl)-benzamide)	1.796	1.757	0.039	1.465	0.331
70	CH	3-(<i>N</i> -(2-Pyrrolidin-1-yl-ethyl)-benzamide)	1.745	1.693	0.052	1.846	−0.101
71	CH	3-(4-Methyl-piperazine-1-sulfonyl)	0.495	0.302	0.193	0.735	−0.240
72	N	3-(2-Pyrrolidin-1-yl-ethoxy)	2.194	2.361	−0.167	1.997	0.197
73	CH	4-(4-Methyl-piperazine-1-sulfonyl)	0.863	0.891	−0.028	1.208	−0.345
74	CH	3-(Piperazine-1-sulfonyl)	0.319	0.370	−0.051	0.751	−0.432
75	CH	4-(Piperazine-1-sulfonyl)	0.893	0.909	−0.016	1.158	−0.265
76	CH	3-(<i>N,N</i> -Dimethylaminoethyl)sulfonamido	1.387	1.242	0.145	1.310	0.077
77	CH	3-(<i>N,N</i> -Dimethylaminopropyl)sulfonamido	1.538	1.395	0.143	1.296	0.242
78	CH	4-(<i>N,N</i> -Dimethylaminoethyl)sulfonamido	1.824	2.049	−0.225	1.987	−0.163

^a Biological activity ($\mu\text{mol L}^{-1}$) expressed as $-\log\text{IC}_{50}$ against human Src enzyme.^b Calculated activity from alignment VII.^c Test set molecules.**Figure 1.** Structure of compound **20** and its atoms used for superposition are labeled.

Similarity indices (descriptors) were derived according to Klebe et al.²⁷ with the same lattice box as used in CoMFA calculations. Five CoMSIA similarity index fields available within SYBYL (steric, electrostatic, hydrophobic, hydrogen bond donor, hydrogen bond acceptor) were evaluated using the probe atom. Gaussian-type distance dependence was between the grid point and each atom of the molecule. The default value of 0.3 was used as attenuation factor.

6. Partial least square (PLS) analysis

The method of partial least squares^{38,39} (PLS) implemented in the QSAR module of SYBYL was used to construct and validate the models. Column filtering was set to 2.0 kcal/mol to speed up the analysis and reduce the noise. The CoMFA/CoMSIA descriptors served as independent variables and pIC_{50} values as dependent variable in PLS regression analysis.

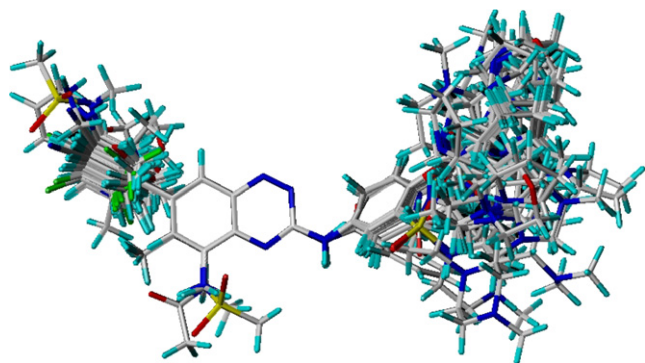


Figure 2. 3D-view of aligned molecules (training and test sets).

Normally, cross-validation is used to check the predictivity of the derived model. Results of the analyses correspond to a regression equation with thousands of coefficients. The performance of models was calculated using the leave one out (LOO) cross-validation method.^{26,40} The optimum number of components (N_c) used to derive the non cross-validated model was defined as the number of components leading to the highest R^2 cross-validated (q^2) and lowest standard error of prediction (SEP). To obtain the statistical confidence limits on the analyses, bootstrapping was carried out with 100 groups.

7. Results and discussion

CoMFA and CoMSIA techniques were used to derive 3D-QSAR models on novel series of benzotriazine based compounds acting as Src inhibitors. The biological activity negative logarithm pIC_{50} was used as a dependent variable.

The low energy conformer obtained from the AM1 optimization was used in this study. All compounds were aligned by DATABASE ALIGNMENT method. CoMFA and CoMSIA models were obtained with 72 and 6 molecules in the training and test sets, respectively. Various 3D-QSAR models were generated and the best one was selected based on the statistically significant parameters obtained. The predictive power of the 3D-QSAR models, derived using the training set, was assessed by predicting biological activities of the test set molecules.

The contribution of the steric and electrostatic CoMFA fields (Table 5) yielded a cross-validated $q^2 = 0.526$ with three components, non cross-validated R^2 of 0.781, F

value 88.132 and bootstrapped R^2 of 0.831. The contribution of the steric and electrostatic fields is 63.1% and 36.9%, respectively. CoMFA contours were generated using this model. The graphs of actual versus fitted and predicted activities for the training and test sets of molecules are depicted in Figure 3.

The field values generated at each grid point were calculated as the scalar product of the associated QSAR coefficient and the standard deviation of all values in the corresponding column of the data table ($\text{STD-DEV} \times \text{COEFF}$), plotted as the percentage contributions to QSAR equation. The CoMFA steric and electrostatic

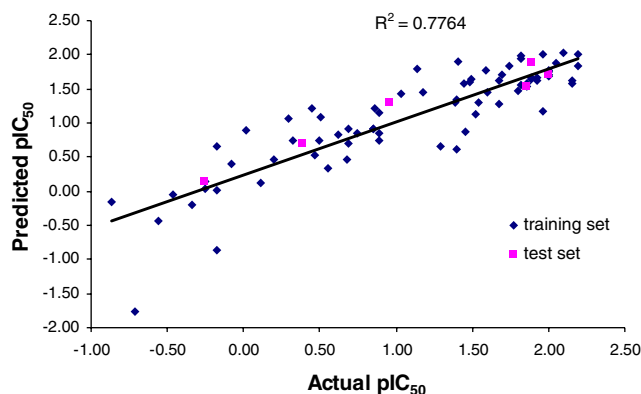


Figure 3. Graph of actual versus calculated activities from CoMFA model.

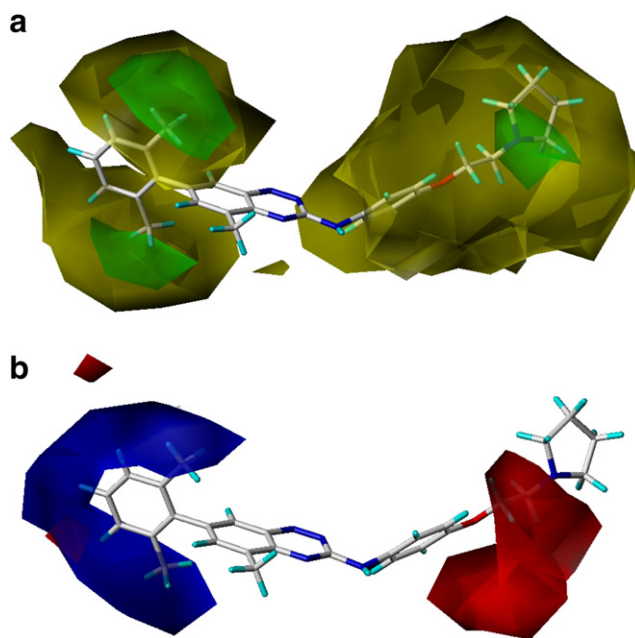


Figure 4. CoMFA STDEV*COEFF contour maps: (a) steric fields; green contours indicate regions where bulky groups increase activity, while yellow contours indicate regions where bulky groups decrease activity, and (b) electrostatic fields; blue contours indicate regions where electropositive groups increase activity, while red contours indicate regions where electronegative groups increase activity. Active Src inhibitor compound **18** is displayed in the background for reference.

Table 5. Summary of CoMFA results

R^2 cross-validated (q^2)	0.526
Standard error of prediction	0.587
Number of components	3
Non cross-validated R^2	0.781
Standard error of estimate	0.399
F value	88.132
R^2_{bs} from 100 bootstrapping runs	0.831
Standard deviation	0.351

Table 6. Summary of CoMSIA results

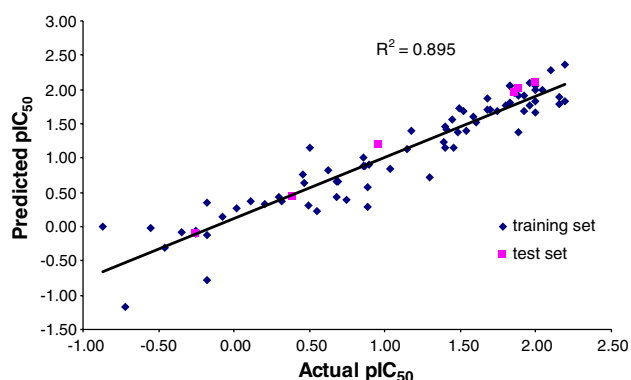
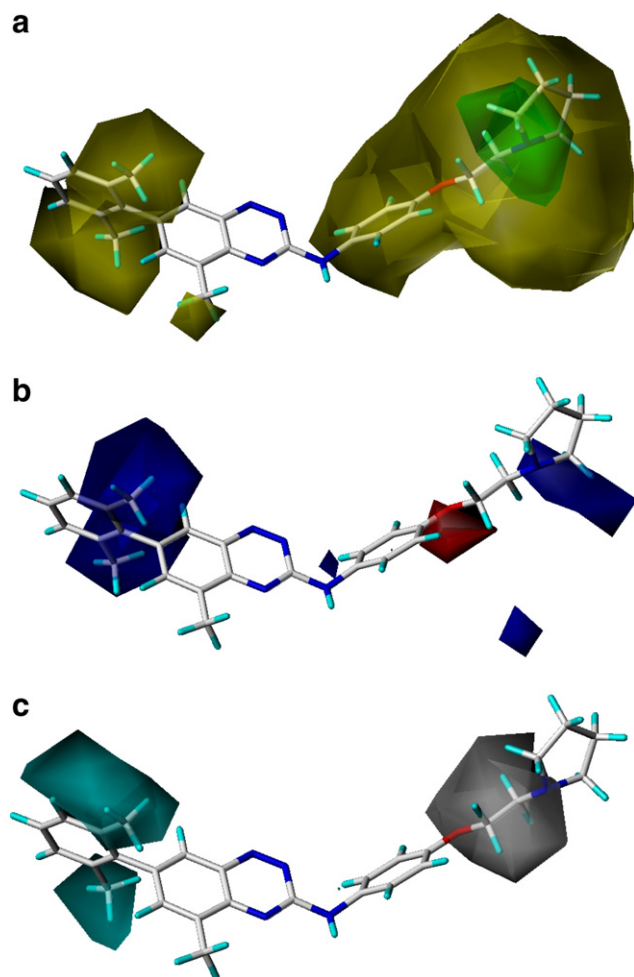
Model	CoMSIA fields	q^2	Nc ^f	SEP ^g	R^2_{ncv} ^h	SEE ⁱ	F value	R^2_{bs} ^j	SD ^k
I	ST ^a , ELE ^b , HFB ^c , DN ^d , AC ^e	0.593	6	0.561	0.919	0.250	127.426	0.950	0.198
II	ST, ELE, HFB, DN	0.589	6	0.564	0.937	0.221	165.593	0.953	0.190
III	ST, ELE, HFB, AC	0.637	5	0.526	0.887	0.293	106.965	0.924	0.241
IV	ST, HFB, DN, AC	0.609	3	0.538	0.789	0.395	87.294	0.826	0.356
V	ST, ELE, DN, AC	0.475	3	0.624	0.784	0.403	62.720	0.762	0.417
VI	ELE, HFB, DN, AC	0.570	7	0.582	0.943	0.211	156.336	0.961	0.172
VII	ST, ELE, HFB	0.647	5	0.519	0.895	0.283	115.906	0.953	0.178
VIII	ST, HFB, DN	0.612	5	0.544	0.880	0.302	99.874	0.920	0.250
IX	ELE, HFB, DN	0.556	5	0.582	0.899	0.278	120.852	0.927	0.235
X	ELE, HFB, AC	0.599	5	0.553	0.876	0.308	96.104	0.912	0.256

^a Steric field.^b Electrostatic field.^c Hydrophobic field.^d Donor field.^e Acceptor field.^f Standard error of prediction.^g Number of components.^h Non cross-validated square of correlation coefficient.ⁱ Standard error of estimate.^j From 100 bootstrapping runs.^k Standard deviation.

contour maps developed are shown in Figure 4a and b, respectively.

The CoMFA steric map encompasses sterically unfavorable contours (20% contribution) corresponding to regions in space where steric bulk envisages the decrease in activity and the polyhedron bordering the groups around 3'- and 7'-positions of benzotriazine ring suggests that bulkier substituents are not favorable in those regions. Further, the sterically favorable regions (80% contribution) observed inside of the steric unfavorable regions in the vicinity of 7-phenyl ring of compound **18** reveal that an increase in activity is matching by medium-size steric bulks substituents such as 2,6 dimethyl phenyl group (Tables 1, 2, and 4).

The CoMFA electrostatic map (Fig. 4b) displays contours in the vicinity of the oxygen linker where the partial negative charge is associated with electronegative substituents and increased activity (20% contribution). Contours observed in the vicinity of 7-dimethyl phenyl group of benzotriazine ring (80% contribution) of com-

**Figure 5.** Graph of actual versus predicted activities from CoMSIA with steric, electrostatic, and hydrophobic fields.**Figure 6.** CoMSIA STDEV*COEFF contour maps: (a) steric, (b) electrostatic, and (c) hydrophobic fields; lipophilic contour plots: cyan contours (80% contribution) and white contours (20% contribution) show regions where an increase in lipophilicity or hydrophilicity, respectively, will enhance activity. Active Src inhibitor compound **18** is displayed in the background for reference.

pound **18** point out areas where the electropositive properties of molecules indicate low electron density and an increase in activity.

In addition to steric and electrostatic fields, CoMSIA also defines the lipophilicity, hydrogen bond donor and acceptor fields that are not generally accessible with standard CoMFA.

The CoMSIA model I with the combinations of all fields (Table 6) yielded a cross-validated $q^2 = 0.593$ with six components, non cross-validated R^2 of 0.919, F value of 127.426, and bootstrapped R^2 of 0.950. The contributions of the steric, electrostatic, hydrophobic, hydrogen bond donor, and acceptor fields of this model were 14.0%, 27.5%, 23.9%, and 34.6%, respectively.

The CoMSIA model with the combinations of steric, electrostatic, and hydrophobic fields (model VII) yielded the highest cross-validated $q^2 = 0.647$ with five components, non cross-validated R^2 of 0.895, F value of 115.906 and bootstrapped R^2 of 0.953. The steric, electrostatic and hydrophobic fields contributions were 27.5%, 32.0%, and 40.5%, respectively. The graph of the actual versus predicted biological activities for the molecules is shown in Figure 5.

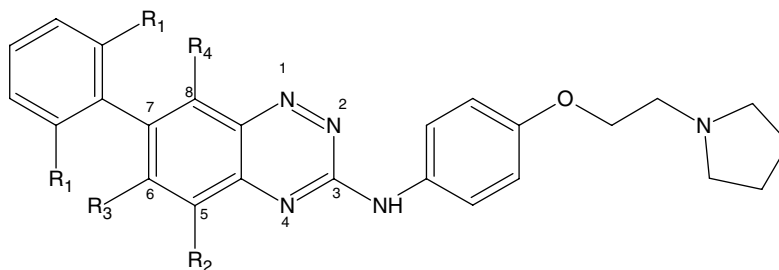
Combinations of electrostatic, hydrophobic, and hydrogen bond donor fields (model IX) yield a cross-validated

$q^2 = 0.556$ with five components, non cross-validated R^2 of 0.899, F value of 120.852, and bootstrapped R^2 of 0.927. The electrostatic, hydrophobic, and donor hydrogen bond fields contributions were 34.4%, 43.4%, and 22.2%, respectively.

The models generated by various combinations of CoMSIA fields (Table 6) show statistical significance, moderate to high, internal and external predictions and a high degree of confidence in the analyses performed, in which the steric, electrostatic and hydrophobic fields were observed to be predominant over the hydrogen bond donor and acceptor fields.

The CoMSIA steric contour was positioned almost similarly, whereas the electrostatic contour was quite different to those of the CoMFA model. The contour maps of CoMSIA (STDDEV*COEFF) are displayed in Figure 6. It is observed that yellow-colored three-dimensional contour surfaces for the steric field, Figure 6a, spread along the aromatic moiety where the presence of atoms or small groups as the chlorine and the methyl implies an increase of the inhibitory activity. Notably, the spatial location of the methyl substituent groups of the ring of benzene on the left moiety of the molecule coincides with that of the blue polyhedrons generated from CoMSIA that show the electrostatic field, Figure 6b, by means of areas where electron-donating groups increase the biological activity. Methyl is an electron-releasing

Table 7. Proposed Compounds based on CoMSIA model



Compound	R ₁	R ₂	R ₃	R ₄	CoMSIA
18	<i>Me</i>	<i>Me</i>	<i>H</i>	<i>H</i>	1.887
79	Me	Me	Me	H	1.996
80	Me	Me	H	Me	1.982
81	Me	Me	Et	H	2.138
82	Me	Et	Me	H	2.074
83	Me	Et	Et	H	2.182
84	Me	Me	Me	Me	2.050
85	Me	Me	Et	Me	2.207
86	Me	Et	Me	Me	2.143
87	Me	Et	Et	Me	2.245
20	<i>Cl</i>	<i>Me</i>	<i>H</i>	<i>H</i>	1.777
88	Cl	Me	Me	H	1.416
89	Cl	Me	H	Me	1.904
90	Cl	Me	Et	H	2.197
91	Cl	Et	Me	H	2.112
92	Cl	Et	Et	H	2.239
93	Cl	Me	Me	Me	1.971
94	Cl	Me	Et	Me	2.269
95	Cl	Et	Me	Me	2.174
96	Cl	Et	Et	Me	2.306

Compounds **18** and **20** are italicized for reference.

group which places increasing electronic density into the ring making it easier for electrophilic attacks. In compound **20** (Table 2) it is noted that when bearing chlorine atoms two phenomena acting in opposite sense take place leading to only a slight modification of the IC₅₀ value of the compound. For one, chlorides would tend to diminish the activity for their electron-withdrawing effect. On the other hand, they increase the biological activity for being located in a yellow area of the CoMSIA steric field.

The cyan-colored contours covering the hydrophobic moiety of the ligands (the vicinity of 7-phenyl ring), Figure 6c, correspond to lipophilic chemical functions that in docking studies had been demonstrated that they interact with the residues of the hydrophobic cavity.^{24,25} Similarly, the presence of partially polar groups such as 3-NHMe Ph (**45**); 3-Cl, 6-OMe Ph (**25**); 2-pyrimidyl (**29**), among others, leads to a decrease in the biological activity of these compounds, due to the hydrophobicity of the cavity likely by means of hydrophobe versus polar repulsions. On the other hand, the contour region (20% contribution) around 2-pyrrolidin-1-ylethoxy group, solvent accessible region, indicates that hydrophilic substituents will enhance activity. The replacement of the ether linkage in **18** with sulfonamide or amide groups resulted in **37** (Table 3), **69** and **70** (Table 4), respectively, with comparable potency to **18** due to the fact that these linkers are in regions where electronegative (Fig. 6b) and hydrophilic (Fig. 6c) substituents increase activity.

The present results of 3D-QSAR studies are in agreement with the in vitro Src inhibitory activity as was reported by Noronha et al.^{24,25}

Regarding the outliers in the regression line, Figures 3 and 5, their structures had been randomly designed before the authors²⁴ found a structural pattern consistent with a suitable inhibitory activity. Later some appropriated features were established²⁵ which led to greater regularity in the architecture of the molecules allowing the generation of a QSAR model sufficiently robust. Furthermore, as long as the biological activity increases the points fit good enough to our regression line.

By comparing the structure of the compounds **7** and **8**, it is observed that the difference lies in an extra methyl group added in the position 6 of the nucleus of benzotriazine in the compound **8**, which increases the pIC₅₀ activity from 0.387 to 0.886, respectively. Based on this observation, we proposed in this paper new compounds derived from the ligands **18** and **20**. These new proposed compounds were generated by combining substituents on the positions 5, 6, and 8 of the benzotriazine nucleus and it was further evaluated the way in which the tested changes affect the inhibitory activity. For this evaluation the CoMSIA model was used since it demonstrated to be more robust than the CoMFA model. The results are shown in Table 7. The hydrogens of the alkyl substituents, of the structures here generated, are close to the yellow contours of the steric field where nonvoluminous groups increase the biological activity. Interestingly, the ethyl group added at the position 6 of the

benzotriazine nucleus, Figure 7, is located in the cyan and yellow contours of the hydrophobic and steric fields, respectively, which helps to explain the high potency predicted by CoMSIA.

Future studies will focus on the design and improvement of new ligands using de novo design tools, as well as ligand–protein flexible docking, in order to achieve a better understanding of the processes of molecular recognition involved in these benzotriazine derived series.

8. Conclusions

A receptor independent 3D-QSAR has been established for benzotriazine based compounds as Src inhibitors

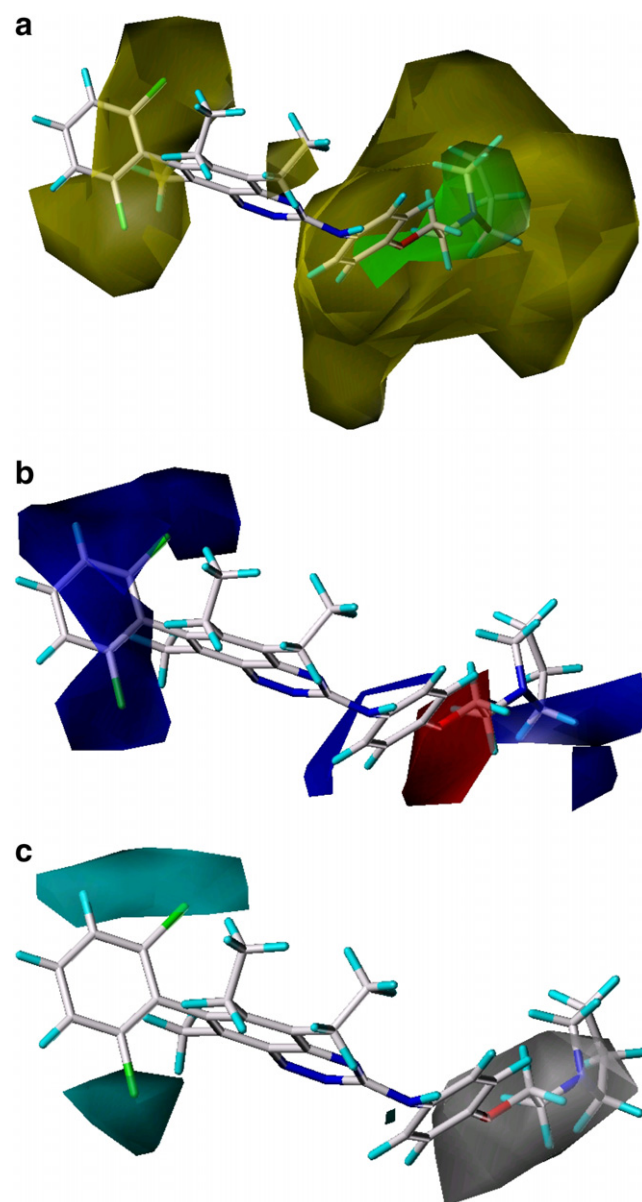


Figure 7. CoMSIA STDEV*COEFF contour maps: (a) steric, (b) electrostatic, and (c) hydrophobic fields around the proposed compound **96**.

employing the most widely used techniques CoMFA and CoMSIA. The present studies highlight the importance of ligand orientation and selection of the training set molecules in the development of statistically significant QSAR models. CoMSIA models provided better statistical models than CoMFA, which points to the significance of hydrophobic field in activity of these ligands in addition to steric and electrostatic fields. The statistical significance and robustness of generated 3D-QSAR models were confirmed using an external set of molecules. The structural requirements identified in the present studies were used to propose new compounds carrying out substitutions at positions 5, 6, and 8 of the benzotriazine nucleus which yielded greater potency than the original ones. Herein our model can be used strategically in the design of novel, potent, and selective Src inhibitors as anticancer therapeutic agents.

References and notes

- Taylor, S. J.; Shalloway, D. *Bio. Essays* **1996**, *18*, 9.
- Thomas, S. M.; Brugge, J. S. *Annu. Rev. Cell. Dev. Biol.* **1997**, *13*, 513.
- Frame, M. C. *J. Cell Sci.* **2004**, *117*, 989.
- Yeatman, T. J. *Nat. Rev. Cancer* **2004**, *4*, 470.
- Verbeek, B. S.; Vroom, T. M.; Adriaansen-Slot, S. S.; Ottenhoff-Kalff, A. E.; Geertzema, J. G.; Hennipman, A.; Rijksen, G. *J. Pathol.* **1996**, *180*, 383.
- Egan, C.; Pang, A.; Durda, D.; Cheng, H. C.; Wang, J. H.; Fujita, D. *J. Oncogene* **1999**, *18*, 1227.
- Bolen, J. B.; Veillette, A.; Schwartz, A. M.; DeSeau, V.; Rosen, N. *Proc. Natl. Acad. Sci. U.S.A.* **1987**, *84*, 2251.
- Cartwright, C. A.; Meisler, A. I.; Eckhart, W. *Proc. Natl. Acad. Sci. U.S.A.* **1990**, *87*, 558.
- Irby, R. B.; Mao, W.; Coppola, D.; Kang, J.; Loubeau, J. M.; Trudeau, W.; Karl, R.; Fujita, D. J.; Jove, R.; Yeatman, T. J. *Nat. Genet.* **1999**, *21*, 187.
- Lutz, M. P.; Esser, I. B.; Flossmann-Kast, B. B.; Vogelmann, R.; Luhrs, H.; Friess, H.; Buchler, M. W.; Adler, G. *Biochem. Biophys. Res. Commun.* **1998**, *243*, 503.
- Visser, C. J.; Rijksen, G.; Woutersen, R. A.; De Weger, R. A. *Lab. Invest.* **1996**, *74*, 2.
- Warmuth, M.; Damoiseaux, R.; Liu, Y.; Fabbro, D.; Gray, N. *Curr. Pharm. Des.* **2003**, *9*, 2043.
- Boschelli, D. H.; Wu, B.; Sosa, A. C. B.; Durutlic, H.; Ye, F.; Raifeld, Y.; Golas, J. M.; Boschelli, F. *J. Med. Chem.* **2004**, *47*, 6666.
- Boschelli, D. H.; Wu, B.; Sosa, A. C. B.; Durutlic, H.; Chen, J. J.; Wang, Y.; Golas, J. M.; Lucas, J.; Boschelli, F. *J. Med. Chem.* **2005**, *48*, 3891.
- Boschelli, D. H.; Wu, B.; Sosa, A. C. B.; Chen, J. J.; Golas, J. M.; Boschelli, F. *Bioorg. Med. Chem. Lett.* **2005**, *15*, 4681.
- Manetti, F.; Locatelli, G. A.; Maga, G.; Schenone, S.; Modugno, M.; Forli, S.; Corelli, F.; Botta, M. *J. Med. Chem.* **2006**, *49*, 3278.
- Carraro, F.; Naldini, A.; Pucci, A.; Locatelli, G. A.; Maga, G.; Schenone, S.; Bruno, O.; Ranise, A.; Bondavalli, F.; Brullo, C.; Fossa, P.; Menozzi, G.; Mosti, L.; Modugno, M.; Tintori, C.; Manetti, F.; Botta, M. *J. Med. Chem.* **2006**, *49*, 1549.
- Dalgarno, D.; Stehle, T.; Narula, S.; Schelling, P.; van Schravendijk, M.; Adams, S.; Andrade, L.; Keats, J.; Ram, M.; Jin, L.; Grossman, T.; MacNeil, I.; Metcalf, C.; Shakespeare, W.; Wang, Y.; Keenan, T.; Sundaramoorthi, R.; Bohacek, R.; Weigle, M.; Sawyer, T. *Chem. Biol. Drug Des.* **2006**, *67*, 46.
- Wang, Y.; Metcalf, C.; Shakespeare, W.; Sundaramoorthi, R.; Keenan, T.; Bohacek, R.; Van Schravendijk, M.; Violette, S.; Narula, S.; Dalgarno, D.; Haraldson, C.; Keats, J.; Liou, S.; Mani, U.; Pradeepan, S.; Ram, M.; Adams, S.; Weigle, M.; Sawyer, T. *Bioorg. Med. Chem. Lett.* **2003**, *13*, 3067.
- Honold, K.; Kaluza, K.; Masjost, B.; Schaefer, W.; Scheiblich, S. Hoffmann-La Roche, WO2006066913, 2006.
- Dow, R. L.; Bechle, B. M.; Chou, T. T.; Goddard, C.; Larson, E. R. *Bioorg. Med. Chem. Lett.* **1995**, *5*, 1007.
- Hanke, J. H.; Gardner, J. P.; Dow, R. L.; Changelian, P. S.; Brissette, W. H.; Weringer, E. J.; Pollok, B. A.; Connolly, P. A. *J. Biol. Chem.* **1996**, *271*, 695.
- Myers, M. R.; Setzer, N. N.; Spada, A. P.; Zulli, A. L.; Hsu, C.-Y. J.; Zilberstein, A.; Johnson, S. E.; Hook, L. E.; Jacoski, M. V. *Bioorg. Med. Chem. Lett.* **1997**, *7*, 417.
- Noronha, G.; Barrett, K.; Cao, J.; Dneprovskaia, E.; Fine, R.; Gong, X.; Gritzen, C.; Hood, J.; Kang, X.; Klebansky, B.; Lohse, D.; Mak, C. C.; McPherson, A.; Palanki, M. S. S.; Pathak, V. P.; Renick, J.; Soll, R.; Splittgerber, U.; Wrasidlo, W.; Zeng, B.; Zhao, N. *Bioorg. Med. Chem. Lett.* **2006**, *16*, 5546.
- Noronha, G.; Barrett, K.; Boccia, A.; Brodhag, T.; Cao, J.; Chow, C.; Dneprovskaia, E.; Doukas, J.; Fine, R.; Gong, X.; Gritzen, C.; Gu, H.; Hanna, E.; Hood, J.; Hu, S.; Kang, X.; Key, J.; Klebansky, B.; Kousba, A.; Li, G.; Lohse, D.; Mak, C. C.; McPherson, A.; Palanki, M. S. S.; Pathak, V. P.; Renick, J.; Shi, F.; Soll, R.; Splittgerber, U.; Stoughton, S.; Tang, S.; Yee, S.; Zeng, B.; Zhao, N.; Zhu, H. *Bioorg. Med. Chem. Lett.* **2007**, *17*, 602.
- Cramer, R. D., III; Patterson, D. E.; Bunce, J. D. *J. Am. Chem. Soc.* **1988**, *110*, 5959.
- Klebe, G.; Abraham, U.; Mietzner, T. *J. Med. Chem.* **1994**, *37*, 4130.
- Bohm, M.; Sturzebecher, J.; Klebe, G. *J. Med. Chem.* **1999**, *42*, 458.
- Bursi, R.; Sawa, M.; Hiramatsu, Y.; Kondo, H. *J. Med. Chem.* **2002**, *45*, 781.
- Sun, W. S.; Park, Y. S.; Yoo, J.; Park, K. D.; Kim, S. H.; Kim, J. H.; Park, H. J. *J. Med. Chem.* **2003**, *46*, 5619.
- Kuo, C. L.; Assefa, H.; Kamath, S.; Brzozowski, Z.; Slawinski, J.; Saczewski, F.; Buolamwini, J. K.; Neamati, N. *J. Med. Chem.* **2004**, *47*, 385.
- SYBYL Molecular Modeling System, version 7.0, Tripos Inc., St. Louis, MO, 63144-2913.
- Clark, M.; Cramer, R. D.; Opdenbosch, N. V. *J. Comput. Chem.* **1989**, *10*, 982.
- Gasteiger, J.; Marsili, M. *Tetrahedron* **1980**, *36*, 3219.
- Dewar, M. J. S.; Zoebisch, E. G.; Healy, E. F.; Stewart, J. J. P. *J. Am. Chem. Soc.* **1985**, *107*, 3902.
- Gaussian 98, Revision B.02. Gaussian, Inc., Pittsburgh, PA, 1995.
- Zou, X.; Lai, L.; Jin, G.; Zhang, Z. *J. Agric. Food Chem.* **2002**, *50*, 3757.
- Wold, S.; Albano, C.; Dunn, W.; Edlund, U.; Esbensen, K.; Geladi, P.; Hellberg, S.; Johansson, E.; Lindberg, W.; Sjostrom, M. In *Chemometrics*; Kolwalski, B., Ed.; Reidel: Dordrecht, 1987; Vol. 1, p 17.
- Geladi, P. *J. Chemom.* **1998**, *2*, 231.
- Wold, S. *Technometrics* **1978**, *4*, 397.